River restoration works design based on the study of early-stage vegetation development and alternate bar dynamics

Li, Jiaze; Claude, Nicolas; Tassi, Pablo; Cordier, Florian; Crosato, Alessandra; Rodrigues, Stéphane

DOI
10.1002/rra.4188

Publication date
2023

Document Version
Final published version

Published in
River Research and Applications

Citation (APA)
Li, J., Claude, N., Tassi, P., Cordier, F., Crosato, A., & Rodrigues, S. (2023). River restoration works design based on the study of early-stage vegetation development and alternate bar dynamics. *River Research and Applications*, *39*(9), 1682-1695. https://doi.org/10.1002/rra.4188

Received: 16 December 2022 | Revised: 12 June 2023 | Accepted: 3 July 2023

DOI: 10.1002/rra.4188

RESEARCH ARTICLE

WILEY

River restoration works design based on the study of early-stage vegetation development and alternate bar dynamics

Jiaze Li[1,2,3] | Nicolas Claude[4] | Pablo Tassi[1,2] | Florian Cordier[1] | Alessandra Crosato[5,6] | Stéphane Rodrigues[3,7]

[1]EDF R&D – National Laboratory for Hydraulics and Environment (LNHE), Chatou, France

[2]Saint-Venant Laboratory for Hydraulics, Chatou, France

[3]UMR CNRS CITERES, University of Tours, Tours, France

[4]EDF, Hydraulic Engineering Center, La Motte Servolex, France

[5]Faculty of Civil Engineering and Geosciences, Delft University of Technology, Delft, The Netherlands

[6]Department of Water Resources and Ecosystems, IHE Delft Institute for Water Education, Delft, The Netherlands

[7]Graduate School of Engineering Polytech Tours, University of Tours, Tours, France

Correspondence
Jiaze Li, EDF R&D – National Laboratory for Hydraulics and Environment (LNHE), Chatou, France.
Email: l.jiazelu@gmail.com

Funding information
Association Nationale de la Recherche et de la Technologie; Electricité de France; CIFRE, Grant/Award Number: 2019-0514

Abstract

Active geomorphological interventions, such as reprofiling of river bars, are often used to increase bar dynamics and prevent vegetation encroachment. River restoration management should be planned based on the knowledge of what processes will follow the intervention and on the anticipation of the consequences. However, in many cases, the associated physical processes are not clearly identified whereas their consequences on bar morphodynamics are still not fully understood. This study aims to bring new insights into the biomorphodynamics evolution of the riverbed after restoration works by using a 2D biomorphodynamic model developed in the TELEMAC-MASCARET system. It seeks to compare and evaluate the performance of five bar reprofiling scenarios in which the bar elevation is lowered to just below the water level at specified design discharges. The study area is located in the channelized and regulated alpine gravel-bed Isère River (France). Bar dynamics and early stages of vegetation establishment are analyzed for the first 2 years after each restoration scenario. The results indicate that plant colonization would occur in all cases. Overall, maximizing the reduction of bar height is the most effective way to improve the bar dynamics and limit future vegetation encroachment.

KEYWORDS
biomorphodynamic numerical modeling, vegetated bars restoration

1 | INTRODUCTION

Over the centuries, many rivers worldwide have been highly influenced by anthropogenic activities, such as channelization (Mosselman, 2020), hydroelectric power generation (Choi et al., 2005), sediment extraction (Rinaldi et al., 2005), and land-use change (Liébault & Piégay, 2002), resulting in permanent or temporary alterations in their hydrogeomorphic processes. In turn, changes in flow and sediment regimes alter the succession, rejuvenation, and diversity of riparian vegetation (Hupp & Osterkamp, 1996; Solari et al., 2016; Stoffel & Wilford, 2012). For example, plant colonization within channels has been observed in many Alpine rivers following human interventions (Comiti et al., 2011; Serlet et al., 2018), which resulted in local alterations of the water flow and sediment transport (Vargas-Luna et al., 2015). Plants increase the local hydraulic roughness (Stone & Shen, 2002) and reduce the sediment transport capacity (Kothyari et al., 2009), causing bed elevation rise within the vegetated area (Le Bouteiller & Venditti, 2014) and channel narrowing (Gradziński et al., 2003).

Many restoration projects have been developed and carried out from the perspective of riparian vegetation rehabilitation (Webb & Erskine, 2003) or flooding risk prevention (Francalanci et al., 2020). González et al. (2015) examined several works published over the previous 25 years and divided the most commonly used restoration strategies in as follows: (1) *passive*, in which the flow conditions are permanently modified, causing geomorphic changes, as for instance dam removal; and (2) *active*, in which water flow and sediment transport are only temporally altered, as for instance through dam operations and/or geomorphic interventions, such as river bed reprofiling.

However, due to socio-economic or political reasons, active hydrogeomorphic restoration works are often preferred over passive approaches (González et al., 2015; Mürle et al., 2003; Poff & Hart, 2002).

Several studies have described the effects of actively changing the flow regime (e.g., flushing flows), and consequently inducing morphological changes, in riparian vegetation dynamics (Cluett, 2005; Rivaes et al., 2015). Several authors (e.g., Carter Johnson, 2000; Edmaier et al., 2011; Kui & Stella, 2016; Mahoney & Rood, 1998) have shown that seedlings are vulnerable and can die due to prolonged inundation, desiccation, burial, or uprooting. However, Cluett (2005) pointed out that the use of engineered floods for channel maintenance would be largely ineffective in changing river morphology, particularly as a long-term solution. In addition, dam release frequency, intensity, duration, and timing depend not only on environmental restoration goals, but also on stakeholder needs, reservoir management strategies, and socio-economical aspects (Loire et al., 2021).

As an alternative management plan, active geomorphological interventions may be a practical and efficient method for riverbed rehabilitation. For instance, numerous studies have shown how channel widening by floodplain lowering would affect river morphology (Villada Arroyave & Crosato, 2010) and vegetation evolution (Geerling et al., 2008). Janssen et al. (2023) studied the impact of vegetation removal and bar reprofiling on the development of vegetation biodiversity in river channels. Yu et al. (2022) developed a two-dimensional (2D) morphodynamic model of the Bow River in Canada and compared the impact of different bar management strategies on flood mitigation. Their results show that bar removal performs the best in terms of lowering future flood peak levels (Kondolf, 2012). However, most restoration interventions are based on the rule of thumb, with uncertainties about their functioning and effectiveness in time (Van Breen et al., 2003). Therefore, appropriate quantification and optimization of practices toward efficient and durable river restoration remain unclear.

The objective of this study is to bring new insights into the biomorphodynamics evolution of a strongly altered river channel after restoration works using numerical simulations. To this goal, the performance of five different reprofiling strategies is quantified and discussed by analyzing and comparing the bar biomorphological evolution and the temporal–spatial vegetation distribution for 2 years after restoration works. The study area is located within the straightened channelized reach of the Isère River (France). Consistent with the current restoration plan for the Isère River, the target bar level is referred to the water level corresponding to specified design discharges. The 2D biomorphodynamic model simulating flow-sediment-vegetation interactions, previously developed by Jourdain et al. (2020) and Li et al. (2020, 2022), has been adopted for this work and applied to the proposed restoration scenarios.

2 | MATERIALS AND METHODS

2.1 | Study reach

The Isère is a gravel-bed river located in the southeast France Alps (Figure 1a). It is an important tributary of the Rhône River, with a total catchment area of 11,890 km^2 and a length of 286 km. As in many other alpine water courses, anthropic activities have significantly modified the natural state of the river over the last two centuries (Bravard, 1989).

The study area is a 2 km long straightened and channelized reach, located in the Combe de Savoie valley near the city of Fréterive, ending at the confluence with the Arc River (Figure 1b). In this area, the reach-averaged channel width is 100 m and the longitudinal slope is 0.0017 m/m. The river bed is characterized by the presence of alternate bars made of very poorly sorted sediment: the coarsest fraction, with a size larger than 2 mm, has a median diameter of 24 mm, the sand component of 180 µm, whereas the fine component with a size smaller than 63 µm has a median diameter of 50 µm. The mean annual flow is 57 m^3/s, and the 2-year flood and the 10-year flood are 209 and 345 m^3/s, respectively. The main vegetation species that develop on the bars of the Isère River belong to *Salicaceae* (willow) family, such as Salix alba, Salix purpurea, Salix triandra, and Populus nigra (Jourdain, 2017).

Current channel restoration works include vegetation and fine sediment removal, further combined with the reprofiling of bars to increase their dynamics. The most recent interventions were conducted in the winter of 2017–2018, as shown in Figure 1c,d presenting the study reach before and after the restoration works, respectively. The fully vegetated bar that initially appeared in the upstream part of the study reach (Figure 1c) was divided into several central bars by creating secondary channels (Figure 1d), while the changes in bar configuration were smaller in the downstream part of the reach. Bed topography, aerial photography, and flow measurements are being carried out regularly to monitor the effectiveness of the works. Despite the central bar configuration imposed by river managers, alternate bars were observed forming again in 2018 (Figure 1e). This study mainly focuses on the biomorphodynamics evolution of the six alternate bars named from B1 to B6 which are shown in Figure 1e.

2.2 | Biomorphodynamic numerical model

The biomorphodynamic model used in this work is based on the coupling of three modules (Figure 2) of the open-source TELEMAC-MASCARET system. The hydrodynamic module TELEMAC-2D solves the 2D depth-averaged shallow-water equations (de Saint-Venant, 1871; Hervouet, 2007). The sediment transport and morphodynamic module GAIA (Tassi et al., 2023) computes bed level changes based on sediment mass balance (Exner, 1920), with a closure relationship for the sediment transport rate based on the Wilcock and Crowe (2003)'s formula, adapted by Cordier (2018). Interactions between fine and coarse sediments being transported by bedload and suspension, and vegetation have not been considered in this study. Numerical investigations were performed considering only bedload transport and vegetation dynamic mechanisms. Corrections for the direction and magnitude of bedload transport due to bed slope (Flokstra & Koch, 1980; Talmon et al., 1995; van Bendegom, 1947),

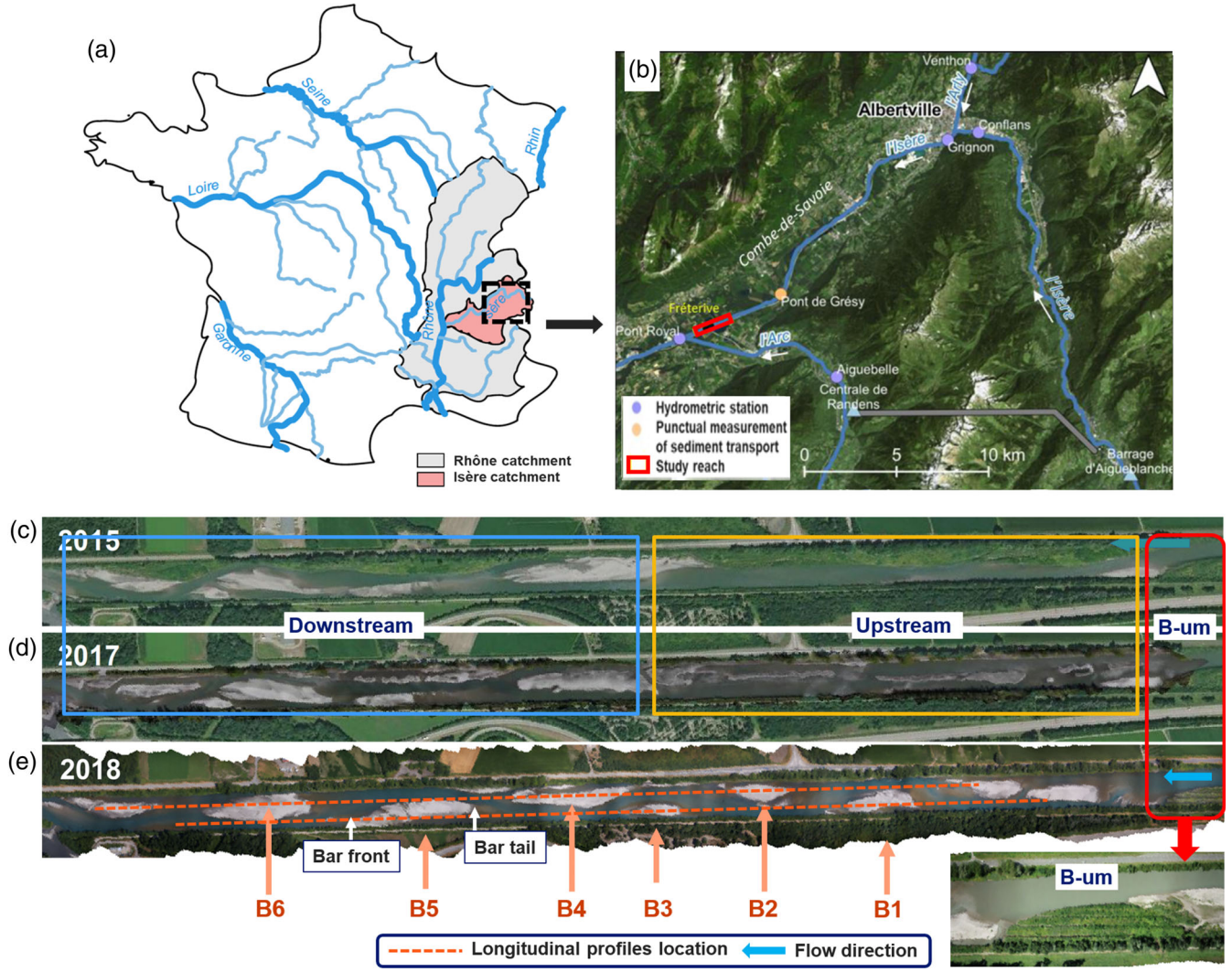

FIGURE 1 Study site: (a) location of Isère catchment in France, (b) location of the study reach in the Combe de Savoie, (c) study reach before restoration works in 2015 and (d) after restoration works in 2017, (e) study reach in 2018 with the reformation of alternate bars. *Source:* Jourdain (2017) and Syndicat Mixte de l'Isère et de l'Arc en Combe de Savoie (SISARC). [Color figure can be viewed at wileyonlinelibrary.com]

skin friction and secondary currents (Engelund, 1974) are incorporated into the morphodynamic model.

The vegetation dynamic module, developed by Jourdain et al. (2020) and Li et al. (2020, 2022), reproduce the main ecological life cycle of vegetation referring to the *Salicaceae familia*, which is dominant over bars of the study reach. The effects of vegetation on hydrodynamics and morphodynamics have been implemented and validated in previous works (Li et al., 2020, 2022). Further details on the full description of the hydromorphodynamic module and implementation of vegetation effects can be found in Li et al. (2022).

Changes in hydromorphological processes can affect vegetation dynamics. Firstly, the recruitment of young seedlings (Figure 2a) including seed dispersal, germination, and survival processes is computed from May to September. Seed dispersal can occur in areas that are not too dry or too wet. Thus, seed dispersal areas can be defined by the minimum and maximum water level recorded from May 1st to July 1st. Consequently, during the germination and growing period from July 1st to September 1st, seedling height follows a linear growth from 0 to 0.45 m until September 1st. Root depth increases following a growth rate of 0.0045 m/day (Guilloy et al., 2011). Meanwhile, seedlings are vulnerable and can die due to prolonged inundation, desiccation, burial, or uprooting (Figure 2a).

Accordingly, for vegetation older than or equal to 1-year old (Figure 2b), plant height h_v (m), root length Lr (m), and stem diameter D_v (m) are modeled according to a logarithmic growth function until the age of 10, as suggested by Oorschot et al. (2016):

$$G = F_v \log[min(Age, 10)] \quad (1)$$

where G represents either the vegetation height h_v, the root length L_r, or the stem diameter D_v. Above, F_v is the growth coefficient related to each variable. In the model, the vegetation characteristics (age, height, diameter, and root length) are updated yearly every September 1st.

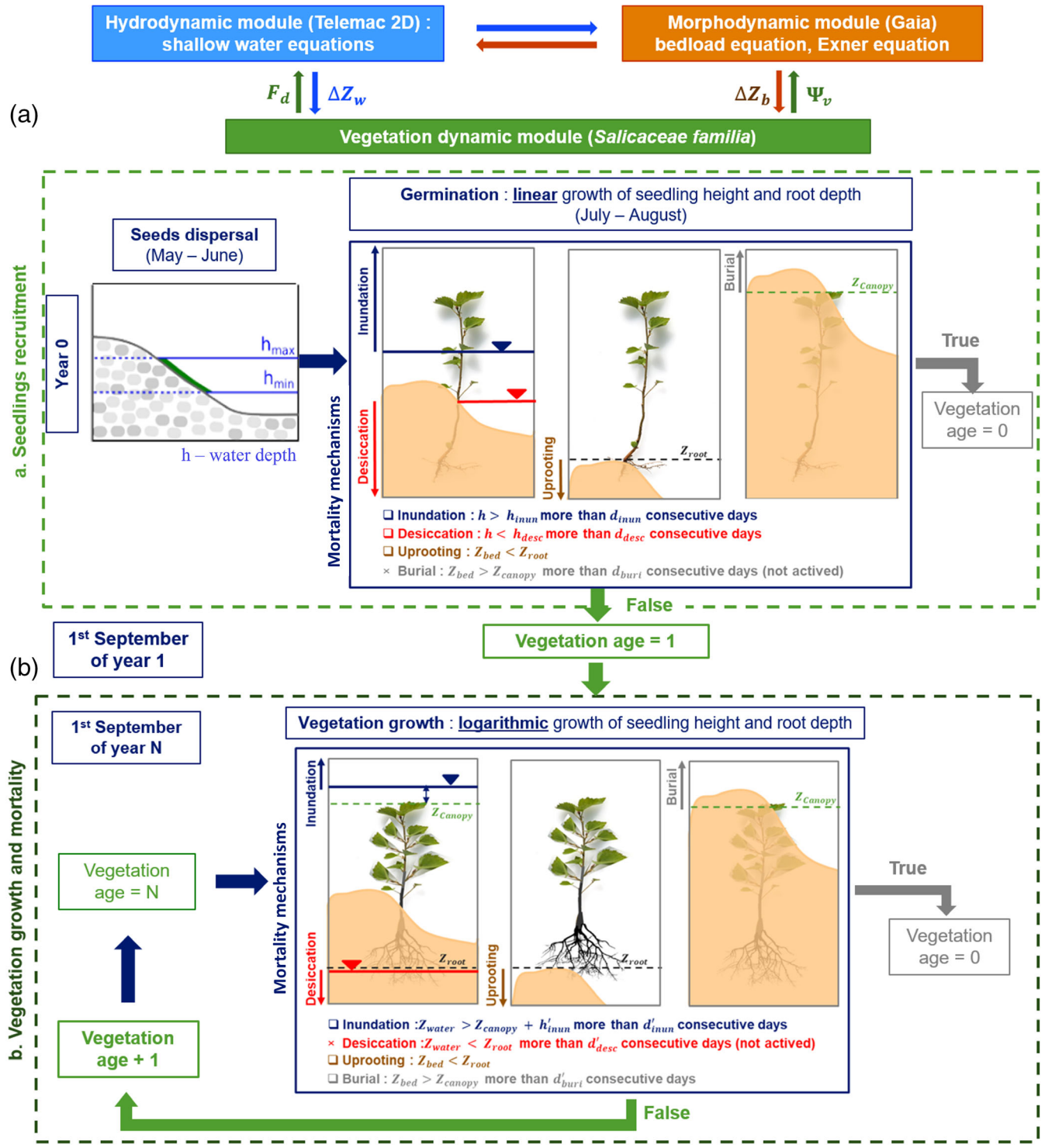

FIGURE 2 Schematic representation of the biomorphodynamic model: (a) seedling recruitment conditions and (b) vegetation growth and mortality. [Color figure can be viewed at wileyonlinelibrary.com]

Established plants can die from different environmental stressors, similar to the seedlings in the recruitment stage, but with higher resistance (Figure 2b). For this, vegetation mortality is also established, related to changes in hydromorphic conditions, at each time step. The full description of the biomorphodynamic model can be found in the Appendix S1.

2.3 | Numerical model set-up and calibration

The computational domain comprises the 2 km study reach sketched in Figure 1 extended upstream and downstream to limit the influence of the boundaries in the study area, for a total length of 4 km. The adopted domain discretization consists of an unstructured finite-

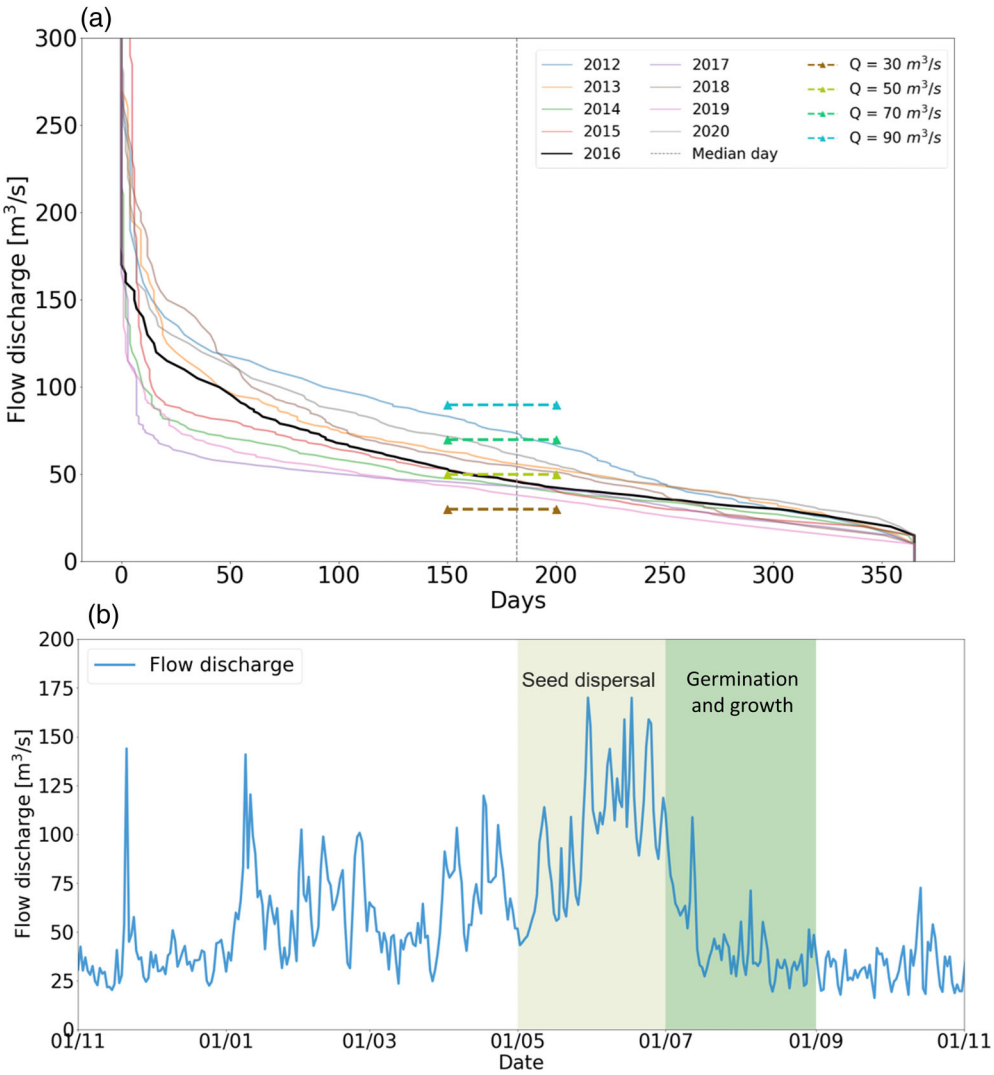

FIGURE 3 (a) Annual flow-duration curves from 2012 to 2020 and (b) flow discharge of 2016 on the study reach. [Color figure can be viewed at wileyonlinelibrary.com]

element mesh composed of 67,508 nodes and 132,498 triangular elements, with an average edge length of 3 m in the study area and 5 m in the extended boundary area. The initial bed elevation is incorporated into the computational mesh from a field measurement survey performed on November 18th, 2020. The time step is set to 0.5 s, resulting in Courant number <1, to guarantee numerical stability, and the total simulation time has been fixed to 2 years. Upstream flow conditions correspond to 2-year repetitions of the discharge measured in 2016, which is the closest to the mean hydrological year estimated over the last 8 years (Figure 3b). The downstream free surface elevation is set up by imposing a stage-discharge rating curve. The bed elevation at the upstream boundary remains constant throughout the simulation and the bed level at the downstream boundary is set as free.

The model considers non-uniform sediment, consisting of two size classes, 0.123 mm and 30 mm, with initial fractions of 11% and 89%. Vegetation characteristics (height, diameter and density) were measured on a restored bar in April 2020 (see Appendix S1). Based on quantitative field measurements of plant height, stem diameter and density of 1–4 years old *Salicaceous* vegetation patches in the study reach, the growth coefficient (Equation 1) for both the vegetation height and root length is assumed to be equal to 2.0 mlog(year)^{-1}, and the one for stem diameter is 0.013 mlog(year)^{-1}. The stem density m is assumed to be constant and equal to 23 steams/m^2. Considering that the study period is limited to the early stage of young seedlings, the change in canopy structure over time is not represented in this study. The calibration procedure was performed to best reproduce the observed changes in the period 2018–2020. More details on the model calibration process and results are provided in the Appendix S1.

2.4 | Numerical scenarios

This study evaluates the effectiveness of lowering the bar height in remobilizing bars and limiting vegetation encroachment. The bar reprofiling operation consists of three steps: (1) determine the target bar top elevation, defined as the submersion level computed for a specific design discharge, (2) compute the volume of sediment that needs to be dug out from each bar and (3) place the excavated gravel in adjacent low-elevation areas (Figure 4).

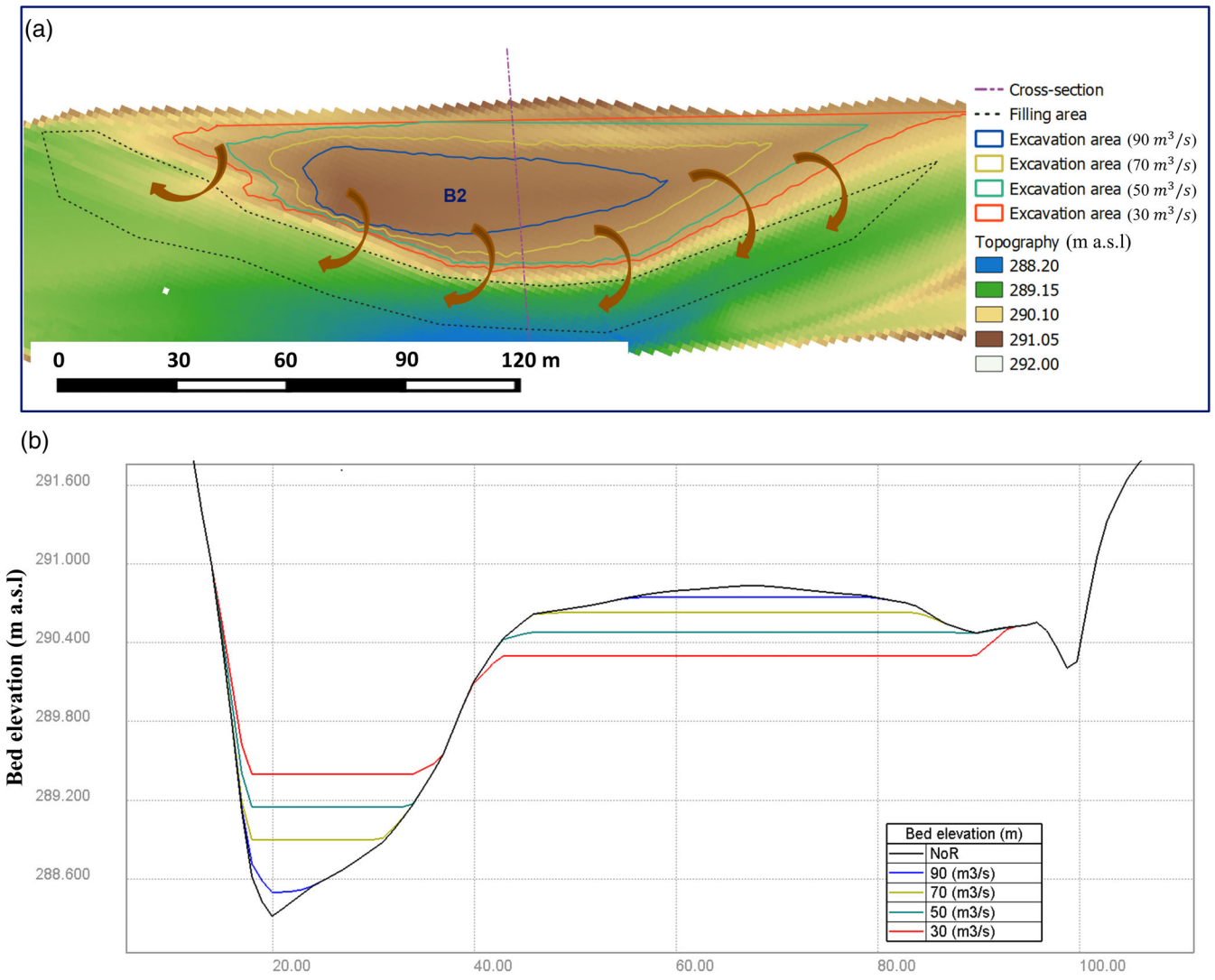

FIGURE 4 (a) Example of excavation and filling areas and (b) bed elevation after the reprofiling along the cross-section for five study scenarios. [Color figure can be viewed at wileyonlinelibrary.com]

A total of five scenarios are considered, corresponding to four design discharges of 30, 50, 70, and 90 m^3/s (respectively R-30, R-50, R-70, and R-90), and one scenario without restoration works (R-NoR), which is defined as the reference scenario. The four design discharges are chosen based on the range of discharges corresponding to the median day of the year (180 days in Figure 3a) for the past 8 years to ensure that bars are submerged most of the time following the restoration work. The target reprofiling elevation of each bar and the corresponding excavation volume is provided in Table S2 in Appendix S1 for each scenario.

2.5 | Data analysis

To characterize and compare the vegetation and alternate bar dynamics obtained for the different scenarios, two longitudinal profiles are extracted at 20 m from both sides of the channel (Figure 1e). These are used to calculate the bar characteristics at the initial and final states of each scenario. In this work, the bar front and bar tail correspond to the downstream and upstream parts of the bars (Figure 1e), respectively. The bar wavelength $L(m)$ is defined by the distance between two consecutive bar fronts and the bar migration is calculated from the location of the front of the same bar at different times (Adami et al., 2016). The bar height $H(m)$ is defined as the difference between the bar top level and the adjacent thalweg level (Eekhout et al., 2013). The analysis of the spatio-temporal vegetation evolution is based on the number of nodes of the computational domain in which the vegetation age is >0 (Figure 2). In addition, the causes of vegetation death are analyzed by first determining the location of "dead" vegetation nodes in which the computed vegetation age has been reset to 0 and by comparing the morphodynamic conditions at the corresponding nodes.

3 | RESULTS

3.1 | Biomorphological evolution of bars

Figures 5 and 6 illustrate the initial and the final bed elevations, the spatial vegetation distribution, and the overall bed evolution for all five scenarios. In addition, bar height, wavelength, and migration distance are calculated to better characterize and compare bar dynamics (Figure 7).

As shown in Figures 5a1 and 6a1, the initial riverbed is almost flat for scenario R-30, in which the restoration work has reached its maximum limit, particularly for bars B1, B3, B4, and B5 with a bar height below 0.1 m (Figure 7a). At the end of the simulation for scenario R-30, a large sediment deposit appears near the right bank opposite the initial location of B1 (Figure 5a2). The initial B1 near the left bank is eroded and transported centrally downstream (Figure 5a3). The tail (upstream) of bar B2 is eroded and its bar front migrates downstream (Figure 5a2,a3). Consecutively, the tails of bars B3 and B4 are eroded as well (Figure 6a2,a3) and their fronts migrate downstream following the channel axis. Finally, in the initial zone of bars B5 and B6, free migrating bars of a shorter wavelength (≈ 300 m) appear (Figure 6a2).

Compared with scenario R-30, which has an almost flat riverbed in the transverse direction, the initial average bar height is 0.6 m in R-50, 1.33 m for the maximum bar height (B2), and 0.25 m for the minimum (B5) (Figure 7a). Similar to scenario R-30, B1 in R-50 migrates downstream to the right bank and merges with the large sediment deposit from upstream, forming a long central bar. B2's tail is also eroded in R-50, but less than observed in R-30 (Figure 5a3,b3) and B2's front migrates downstream. B3 and B4's morphology in R-50 is not significantly different from that in R-30 (Figure 6a2,a3,b2,6b3). However, the initially long bars B5 and B6 are preserved during the simulation time instead of forming bars with shorter wavelengths as observed for R-30. In addition, B5's tail is eroded.

For scenarios R-70, R-90, and R-NoR, less noticeable differences in bar morphology are observed. B1 tends to migrate downstream, but along the left bank (Figure 5c2,d2,e2), rather than along the right bank as in scenarios R-30 and R-50. This induces stronger flow deflection, resulting in a higher B2's tail erosion, compared to R-50 (Figure 5b3,c3,d3,e3). B3 and B4 still present a central configuration but with a more pronounced sinuous main channel (Figure 6c2,d2,e2). B5's tail is eroded in all scenarios, leading to the erosion of B6's tail and side (Figure 6c3,d3,e3).

Overall, the bar height ranges from 2.55 to 2.98 m in scenario R-NoR without reprofiling intervention, from 0.84 to 2.25 m in scenario R-90, from 0.53 m to 1.73 m in R-70, from 0.25 to 1.33 m in R-50 and from 0 to 0.9 m in R-30 (Figure 7a). Despite the reprofiling of bars, the final bar heights increase in all restoration scenarios (R-30 to R-90), as shown in Figure 7b. Initial bar wavelengths range from 437 to 698 m from upstream to downstream, roughly equivalent to 4–7 times the average channel width (Figure 7c), and the final bar wavelengths are more or less shorter than the initial wavelengths, especially for B2 and B5, which are ≈ 180 m shorter. Finally, bar migration is also examined (Figure 7d), and it is found that the bar migration in the upstream part of the reach (100–210 m on average for B1–B4) is greater than the bar migration downstream (≈ 25 m for B5 and B6).

3.2 | Spatial and temporal vegetation dynamics

Figure 8 shows how vegetation has evolved over time and how it is distributed spatially for each numerical scenario. The final results show an overall increasing trend from R-30 to R-NoR, with no significant differences between the R-50 (562 vegetation nodes) and R-70 (566 vegetation nodes) scenarios (Figure 8a). Seedlings mortality in year 1 is observed in all scenarios. About 60 vegetation nodes are lost in scenarios R-90 and R-NoR, while only 2 vegetation nodes disappear in scenario R-30. However, new seedlings colonize bars during the second year, with a minimum of 154 vegetation nodes in scenario R-30 and a maximum of 391 vegetation nodes in scenario R-50.

Regarding the spatial distribution of vegetation (Figure 8b), colonization occurs on most bars in all scenarios, especially on B2, B5, and B6 but with different spatial distributions. For example, in scenario R-30 the vegetation on B2 (Figure 5a2) is distributed along the right bank following a linear tendency, whereas in other scenarios, the vegetation on B2 is primarily distributed in patches in the vicinity of the bar tail (Figure 5b2,c2,d2,e2). The amount of vegetation established on B5 mainly increases from scenario R-70 to R-NoR (Figure 8b), and the corresponding vegetation patch pattern evolves from a stripe patch pattern with vegetation mainly located near the bar front (Figure 6c2,d2) to a filled patch pattern with vegetation mainly located near the bar tail (Figure 6e2). Similarly, for vegetation on B6, its main colonization location tends to shift from the bar front towards the bar tail in scenarios from R50 to R-NoR (Figure 6b2–e2).

Figure 9 illustrates vegetation mortality. As shown in Figure 2b, three possible causes of vegetation mortality are set up in the numerical model: prolonged inundation, burial, and uprooting. Nevertheless, the numerical results show that 1-year-old seedlings die mainly due to uprooting. Mortality by burial is rare and only occurs on bars B2 and B6. No vegetation death due to prolonged inundation is observed in these scenarios.

4 | DISCUSSION

The effects of bar top lowering on limiting vegetation encroachment and re-establishing bar dynamics are evaluated based on the cross-analysis of the results. To facilitate the discussion, design discharges are arbitrarily classified according to the intervention category, where *mild* is referred to discharge values equal to 70 and 90 m^3/s; *moderate*, corresponds to the discharge of 50 m^3/s; and *severe* corresponds to a discharge equal to 30 m^3/s.

Regarding bar dynamics, the bar height tends to increase in all intervention scenarios (Figure 7a,b), whereas the bar wavelength tends to decrease, but mainly for B2 and B5 (Figure 7c). All bar wavelengths range from about 4 to 7 times the average channel width.

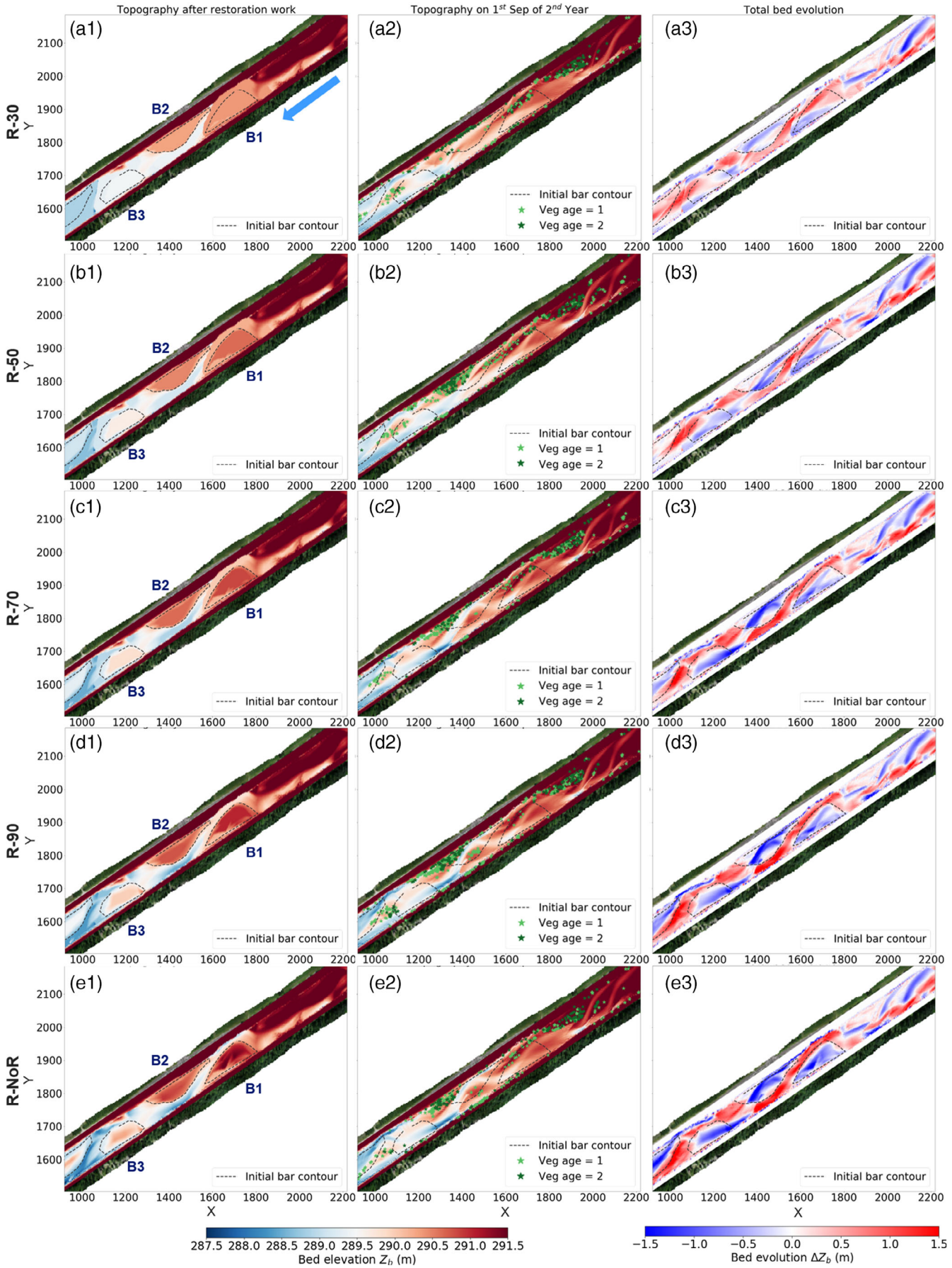

FIGURE 5 Initial bed elevation after restoration work, final bed elevation and vegetation distribution on the September 1st of the second year, and total bed evolution for all scenarios in the upstream part of the study reach. [Color figure can be viewed at wileyonlinelibrary.com]

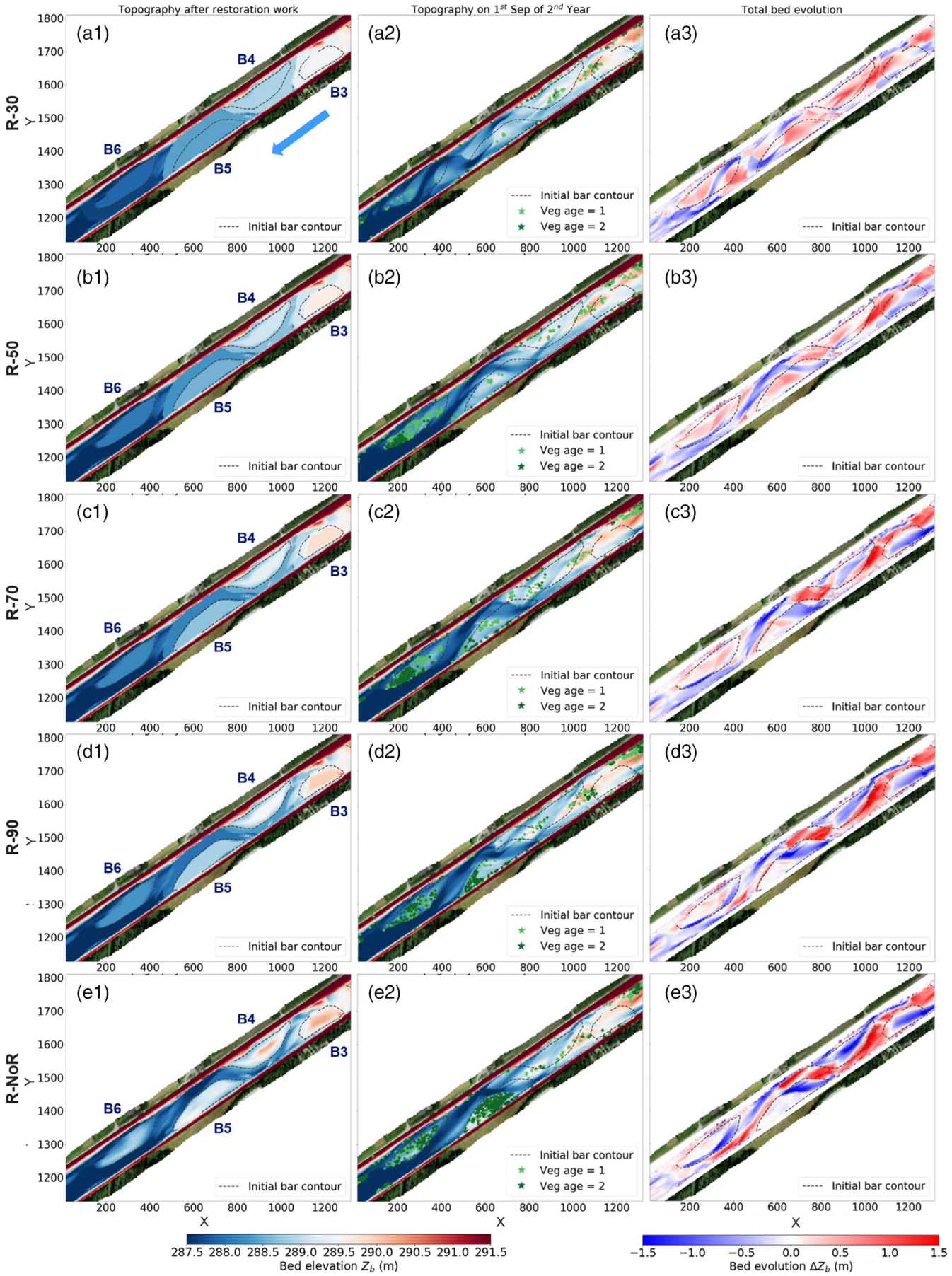

FIGURE 6 Initial bed elevation after restoration work, final bed elevation and vegetation distribution on the September 1st of the second year, and total bed evolution for all scenarios in the downstream part of the study reach. [Color figure can be viewed at wileyonlinelibrary.com]

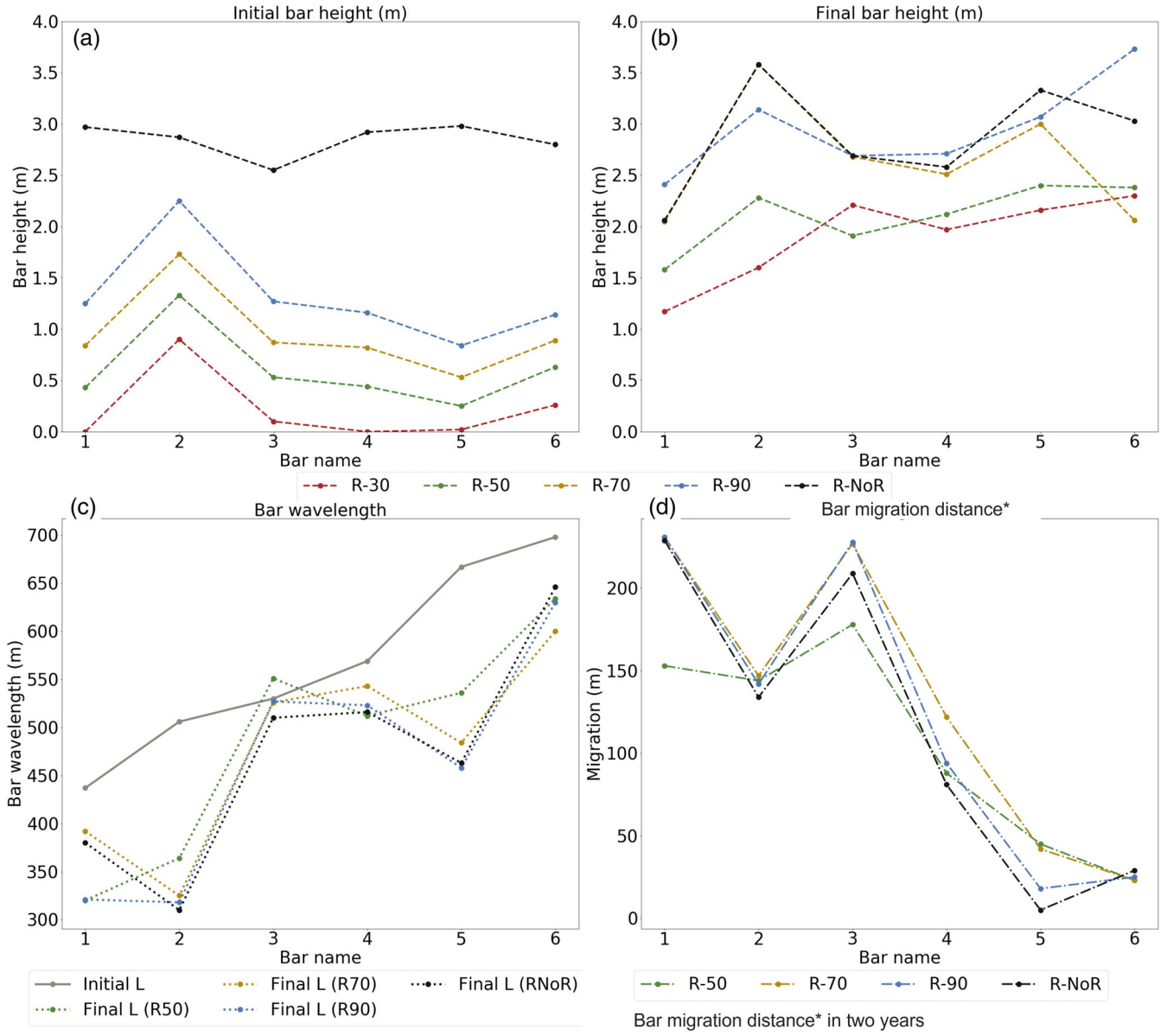

FIGURE 7 (a) Initial and (b) final bar heights, (c) bar wavelengths, and (d) bar migration distances. The final bar wavelength and migration distance for scenario R-30 are not calculated due to the presence of sub-bar unit. [Color figure can be viewed at wileyonlinelibrary.com]

These trends are consistent with the measurements performed by Serlet et al. (2018) on the same study area between 1938 and 1978 when the bars presented little or no vegetation (i.e., in a state close to that obtained post-restoration works).

Overall, for the moderate and severe scenarios (i.e., R-30 and R-50), the bars show similar morphological evolution trends in the upstream part of the reach: the formation of the long central bar B1 near the right bank, as shown in Figure 5a2,b2. Instead, different evolution trends are observed in the downstream part of the reach. Here, scenario R-30 (severe) exhibits shorter bar wavelengths (B5 and B6) than in the moderate scenario (eg. R-50) (Figure 6a2,b2). For the mildest intervention scenarios (e.g., R-70 and R-90), both the bed evolution and the final bed topography are almost identical to the reference scenario without bars reprofiling. An explanation might be that, for the severe scenario, the bar reprofiling results in a relatively flatter riverbed (Figure 7a), with a more uniform flow and bed shear stress distribution along the cross-section (Figures S1 and S2 in Appendix S1) and thus sediment entrainment and transport occurring on the lowered bar tops most of the time. Conversely, for the mild or no-intervention scenarios (ie., R-70, R-90, and R-NoR), the restoration works do not reduce the bar height to the point that the bars are submerged most of the time. This means that most of the time the bed shear stress is not high enough to mobilize the sediment on bar tops so that the bars are less dynamic. This was also observed by Jourdain et al. (2020).

Regarding vegetation dynamics, colonization on bars is obtained for all scenarios after 2 years of evolution. This result is in agreement with the field experiment by Maeno and Watanabe (2008) on a

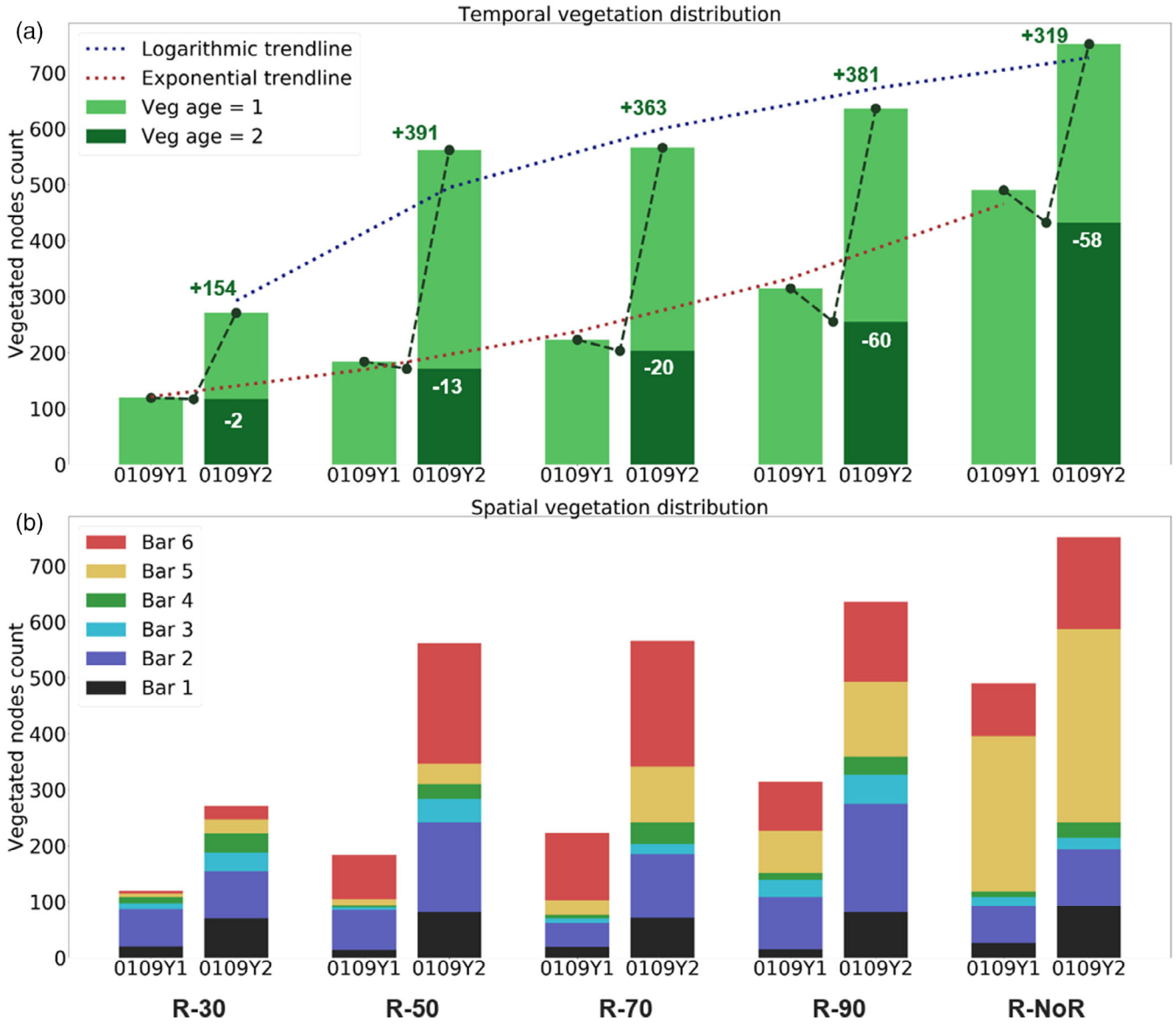

FIGURE 8 (a) Temporal evolution of vegetation and (b) spatial distribution of vegetation on bars. [Color figure can be viewed at wileyonlinelibrary.com]

restored gravel bar in the Asahi River (Japan). The authors showed that Salicaceae species can regenerate rapidly within a year downstream of the restoration area. Our study also shows that the final amount of vegetation varies through the different bar reprofiling scenarios. However, a severe geomorphological intervention, consisting of maximum lowering of the bar top level, might be the most efficient scenario to limit vegetation encroachment on bars.

The final amount of vegetation gradually increases for moderate to severe intervention scenarios (R50, R70, and R90), but with only small differences. Finally, the reference scenario (R-NoR) results in the maximal final amount of vegetation. Indeed, for all scenarios, vegetation is mainly located in B2, B5, and B6 (Figures 5, 6 and 8). Vegetation coverage on B2 differs a little between all scenarios because of the presence of a steady bar nucleus observable in all simulations. On the contrary, the plant coverage varies more significatively for B5 and B6 and explains largely the differences between the different scenarios. For the severe intervention scenario, B5 and B6 become free migrating bars (Figure 6a) which prevent vegetation development on their tops (Figure 9e,f). For moderate and mild interventions, the vegetation develops mainly on B6, which shows low dynamics, and less on B5 with the upstream part that is easily submerged and strongly eroded after the works (Figures 6, 7 and 9e,f). Consequently, the total amount of vegetation in the mild scenarios is greater than in the severe intervention scenario (R30). However, without restoration works (reference scenario) most vegetation develops on both B5 and B6.

Seedling mortality has also been obtained in this study and occurs mainly in B2 and B6 (Figure 9). As also observed by Edmaier et al. (2011), the main cause of mortality is due to Type II uprooting, associated with erosion processes. This is also in agreement with the field

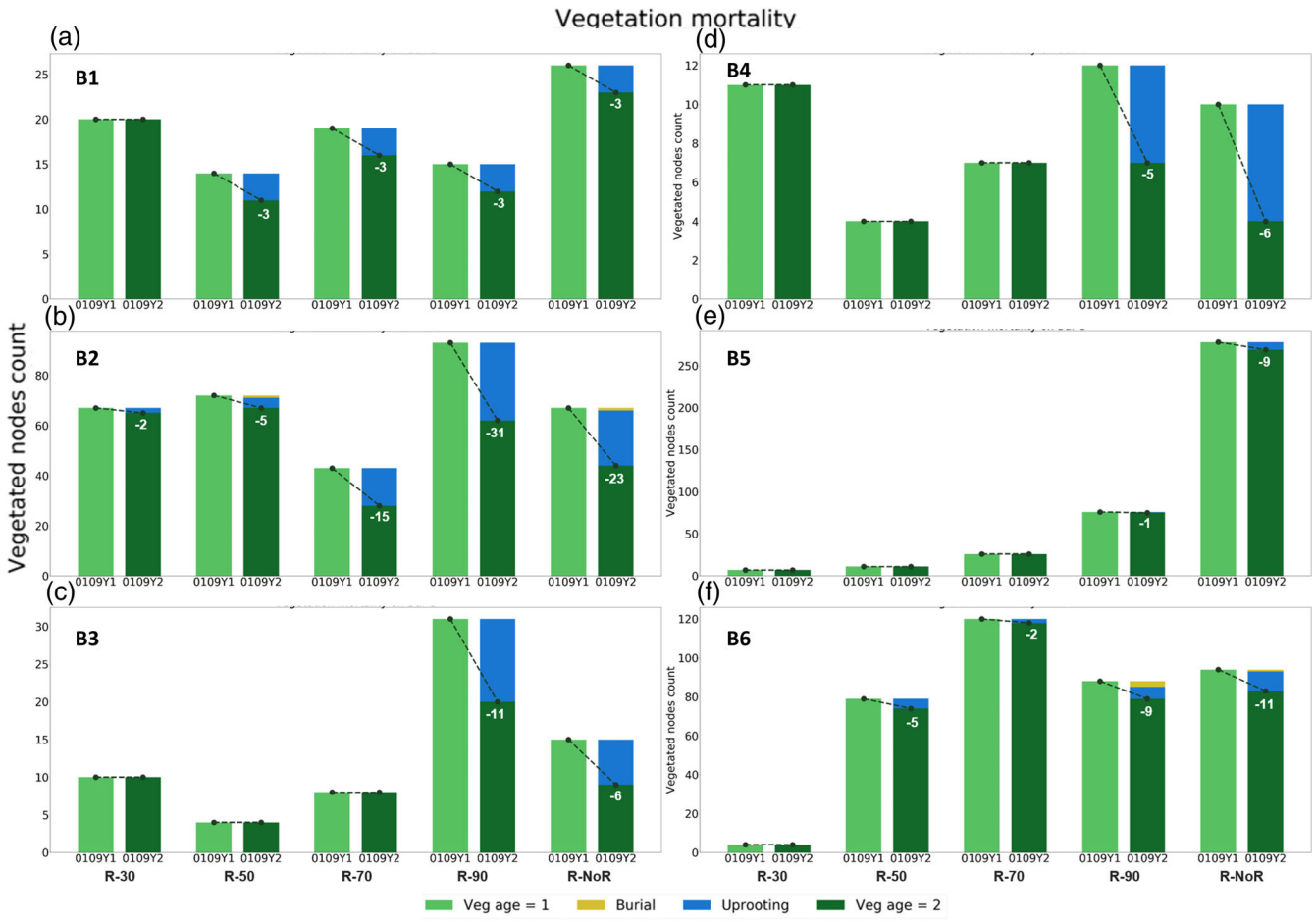

FIGURE 9 Mortality analysis of seedlings established during the first year on bars from B1 to B6. [Color figure can be viewed at wileyonlinelibrary.com]

study of Wintenberger et al. (2019) in the Loire River (France). In general, higher seedling mortality was found in the scenario without intervention (R-NoR), which can be further attributed to higher sediment deposition and erosion (Figures 5e3 and 6e3). Our work is in agreement with the numerical study of Caponi et al. (2020), who showed that the morphodynamic processes play an important role in vegetation dynamics.

Limitations arising from numerical modeling assumptions need to be emphasized. Some important biological processes are not considered in the model, including vegetation establishment and growth related to soil texture, nutrient status or temperature, and ecological processes of inter- or intraspecies competition, promotion, and succession (Bendix & Stella, 2013). In this work, only one hydrological scenario has been tested and the present study focused on the early-stage development of vegetation and bar morphodynamic evolution within 2 years after the restoration. However, flow-sediment-vegetation interactions would be stronger once seedlings become mature trees and the variation in real hydrographs might affect the results obtained in this study. Therefore, the application of the findings of this study to long-term trends should be carefully considered for future research and applications.

5 | CONCLUSIONS

This numerical study compares and evaluates the performance of different alternate bar reprofiling in the Isère River (France) based on bar dynamics and seedling colonization in the 2 years following the restoration works. A 2D biomorphodynamic model is developed and calibrated against field observations. Five different bar reprofiling scenarios are simulated, for which the target bar top level is defined by the water level corresponding to four design discharges. The simulations include a scenario without intervention, the reference scenario.

The results show that plant colonization mainly occurs at the end of the computational time (2 years after the works) for all scenarios. However, the interventions are still found to contribute to the reduction of vegetation encroachment compared to the reference scenario without bar top lowering. It is also found that seedling mortality is mainly due to uprooting, associated with bed erosion processes. This suggests that increasing the bar mobility limits vegetation encroachment. Overall, without considering the restoration budget and complexity of the intervention, this work suggests that leveling the bed as much as possible by minimizing the bar top height may be the most

effective restoration plan. The results show that vegetation tends to colonize steady, stable bars more than migrating bars. This suggests that it may not be always necessary to lower all the bars. It could be more effective to intervene only on the less mobile ones.

ACKNOWLEDGMENTS

The authors would like to acknowledge Electricité de France (EDF) R&D and the French National Association of Research and Technology (ANRT) for funding this research work with the Industrial Conventions for Training through Research (CIFRE grant agreement no. 2019-0514). Coraline Bel is gratefully acknowledged for providing a preliminary version of the hydrodynamics model used in this work.

CONFLICT OF INTEREST STATEMENT

All authors declare that they have no conflicts of interest.

DATA AVAILABILITY STATEMENT

The data that support the findings of this study are available from the corresponding author, N. Claude, upon reasonable request.

ORCID

Jiaze Li https://orcid.org/0000-0003-1643-6792
Nicolas Claude https://orcid.org/0000-0002-0831-1546
Pablo Tassi https://orcid.org/0000-0003-4625-4295
Florian Cordier https://orcid.org/0000-0001-8612-2532
Alessandra Crosato https://orcid.org/0000-0001-9531-005X
Stéphane Rodrigues https://orcid.org/0000-0002-5519-125X

REFERENCES

Adami, L., Bertoldi, W., & Zolezzi, G. (2016). Multidecadal dynamics of alternate bars in the a lpine R hine R iver. *Water Resources Research*, *52*(11), 8938–8955. https://doi.org/10.1002/2015WR018228

Bendix, J., & Stella, J. C. (2013). Riparian vegetation and the fluvial environment: A biogeographic perspective. In *Ecogeomorphology* (pp. 53–74). Elsevier. https://doi.org/10.1016/B978-0-12-374739-6.00322-5

Bravard, J. P. (1989). La métamorphose des rivières des Alpes françaises à la fin du Moyen Âge et à l'époque moderne. *Bulletin de la Société géographique de Liège*, *25*, 145–157. https://popups.uliege.be/0770-7576/index.php?id=3799

Caponi, F., Vetsch, D. F., & Siviglia, A. (2020). A model study of the combined effect of above and below ground plant traits on the ecomorphodynamics of gravel bars. *Scientific Reports*, *10*(1), 1–14. https://doi.org/10.1038/s41598-020-74106-9

Carter Johnson, W. (2000). Tree recruitment and survival in rivers: Influence of hydrological processes. *Hydrological Processes*, *14*(16–17), 3051–3074. https://doi.org/10.1002/1099-1085(200011/12)14:16/17%3C3051::AID-HYP134%3E3.0.CO;2-1

Choi, S. U., Yoon, B., & Woo, H. (2005). Effects of dam-induced flow regime change on downstream river morphology and vegetation cover in the Hwang River, Korea. *River Research and Applications*, *21*(2–3), 315–325. https://doi.org/10.1002/rra.849

Cluett, L. (2005). The role of flooding in morphological changes in the regulated lower Ord River in tropical northwestern Australia. *River Research and Applications*, *21*(2–3), 215–227. https://doi.org/10.1002/rra.842

Comiti, F., Da Canal, M., Surian, N., Mao, L., Picco, L., & Lenzi, M. A. (2011). Channel adjustments and vegetation cover dynamics in a large gravel bed river over the last 200 years. *Geomorphology*, *125*(1), 147–159. https://doi.org/10.1016/j.geomorph.2010.09.011

Cordier, F. (2018). Bars morphodynamics in trained rivers with heterogeneous sediment (Doctoral dissertation, Université Paris-Est). https://hal.archives-ouvertes.fr/tel-02279316/

de Saint-Venant, B. (1871). Theory of unsteady water flow, with application to river floods and to propagation of tides in river channels. *French Academy of Science*, *73*, 148–154.

Edmaier, K., Burlando, P., & Perona, P. (2011). Mechanisms of vegetation uprooting by flow in alluvial non-cohesive sediment. *Hydrology and Earth System Sciences*, *15*(5), 1615–1627. https://doi.org/10.5194/hess-15-1615-2011

Eekhout, J. P. C., Hoitink, A. J. F., & Mosselman, E. (2013). Field experiment on alternate bar development in a straight sand-bed stream. *Water Resources Research*, *49*(12), 8357–8369. https://doi.org/10.1002/2013WR014259

Engelund, F. (1974). Flow and bed topography in channel bends. *Journal of the Hydraulics Division*, *100*(11), 1631–1648. https://doi.org/10.1061/JYCEAJ.0004109

Exner, F. M. (1920). *Zur physik der dünen*. Hölder.

Flokstra, C., & Koch, F. G. (1980). *Bed level computations for curved alluvial channels*. IAHR Congress.

Francalanci, S., Paris, E., & Solari, L. (2020). On the vulnerability of woody riparian vegetation during flood events. *Environmental Fluid Mechanics*, *20*(3), 635–661. https://doi.org/10.1007/s10652-019-09726-5

Geerling, G. W., Kater, E., Van den Brink, C., Baptist, M. J., Ragas, A. M. J., & Smits, A. J. M. (2008). Nature rehabilitation by floodplain excavation: The hydraulic effect of 16 years of sedimentation and vegetation succession along the Waal River, NL. *Geomorphology*, *99*(1–4), 317–328. https://doi.org/10.1016/j.geomorph.2007.11.011

González, E., Sher, A. A., Tabacchi, E., Masip, A., & Poulin, M. (2015). Restoration of riparian vegetation: A global review of implementation and evaluation approaches in the international, peer-reviewed literature. *Journal of Environmental Management*, *158*, 85–94. https://doi.org/10.1016/j.jenvman.2015.04.033

Gradziński, R., Baryła, J., Doktor, M., Gmur, D., Gradziński, M., Kędzior, A., Paszkowski, M., Soja, R., Zielinski, T., & Żurek, S. (2003). Vegetation-controlled modern anastomosing system of the upper Narew River (NE Poland) and its sediments. *Sedimentary Geology*, *157*(3–4), 253–276. https://doi.org/10.1016/S0037-0738(02)00236-1

Guilloy, H., González, E., Muller, E., Hughes, F. M., & Barsoum, N. (2011). Abrupt drops in water table level influence the development of Populus nigra and Salix alba seedlings of different ages. *Wetlands*, *31*(6), 1249–1261. https://doi.org/10.1007/s13157-011-0238-8

Hervouet, J. M. (2007). *Hydrodynamics of free surface flows: Modelling with the finite element method*. John Wiley & Sons.

Hupp, C. R., & Osterkamp, W. R. (1996). Riparian vegetation and fluvial geomorphic processes. *Geomorphology*, *14*(4), 277–295. https://doi.org/10.1016/0169-555X(95)00042-4

Janssen, P., Chevalier, R., Chantereau, M., Dupré, R., Evette, A., Hémeray, D., Marell, A., Martin, H., Rodrigues, S., Villar, M., & Greulich, S. (2023). Can vegetation clearing operations and reprofiling of bars be considered as an ecological restoration measure? Lessons from a 10-year vegetation monitoring program (Loire River, France). *Restoration Ecology*, *31*(3), e13704. https://doi.org/10.1111/rec.13704

Jourdain, C. (2017). Action des crues sur la dynamique sédimentaire et végétale dans un lit de rivière à galets: l'Isère en Combe de Savoie (Doctoral dissertation, Université Grenoble Alpes (ComUE)).

Jourdain, C., Claude, N., Tassi, P., Cordier, F., & Antoine, G. (2020). Morphodynamics of alternate bars in the presence of riparian vegetation. *Earth Surface Processes and Landforms*, *45*(5), 1100–1122. https://doi.org/10.1002/esp.4776

Kondolf, G. M. (2012). The espace de liberté and restoration of fluvial process: When can the river restore itself and when must we intervene? *River Conservation and Management*, 223–241.

Kothyari, U. C., Hashimoto, H., & Hayashi, K. (2009). Effect of tall vegetation on sediment transport by channel flows. *Journal of Hydraulic Research*, *47*(6), 700–710. https://doi.org/10.3826/jhr.2009.3317

Kui, L., & Stella, J. C. (2016). Fluvial sediment burial increases mortality of young riparian trees but induces compensatory growth response in survivors. *Forest Ecology and Management*, *366*, 32–40. https://doi.org/10.1016/j.foreco.2016.02.001

Le Bouteiller, C., & Venditti, J. G. (2014). Vegetation-driven morphodynamic adjustments of a sand bed. *Geophysical Research Letters*, *41*(11), 3876–3883. https://doi.org/10.1002/2014GL060155

Li, J., Claude, N., Tassi, P., Cordier, F., Crosato, A., & Rodrigues, S. (2020). Implementation of a novel approach accounting for the influence of vegetation on sediment transport in GAIA. In *Online proceedings of the papers submitted to the 2020 TELEMAC-MASCARET user conference October 2020* (pp. 2-8).

Li, J., Claude, N., Tassi, P., Cordier, F., Vargas-Luna, A., Crosato, A., & Rodrigues, S. (2022). Effects of vegetation patch patterns on channel morphology: A numerical study. *Journal of Geophysical Research: Earth Surface*, *127*(5), e2021JF006529. https://doi.org/10.1029/2021JF006529

Liébault, F., & Piégay, H. (2002). Causes of 20th century channel narrowing in mountain and piedmont rivers of southeastern France. *Earth Surface Processes and Landforms: The Journal of the British Geomorphological Research Group*, *27*(4), 425–444. https://doi.org/10.1002/esp.328

Loire, R., Piégay, H., Malavoi, J. R., Kondolf, G. M., & Bêche, L. A. (2021). From flushing flows to (eco) morphogenic releases: Evolving terminology, practice, and integration into river management. *Earth-Science Reviews*, *213*, 103475. https://doi.org/10.1016/j.earscirev.2020.103475

Maeno, S., & Watanabe, S. (2008). Field experiment to restore a gravel bar and control growth of trees in the Asahi River. *International Journal of River Basin Management*, *6*(3), 225–232. https://doi.org/10.1080/15715124.2008.9635350

Mahoney, J. M., & Rood, S. B. (1998). Streamflow requirements for cottonwood seedling recruitment—An integrative model. *Wetlands*, *18*(4), 634–645. https://doi.org/10.1007/BF03161678

Mosselman, E. (2020). Studies on river training. *Water*, *12*(11), 3100. https://doi.org/10.3390/w12113100

Mürle, U., Ortlepp, J., & Zahner, M. (2003). Effects of experimental flooding on riverine morphology, structure and riparian vegetation: The river Spöl, Swiss National Park. *Aquatic Sciences*, *65*, 191–198.

Oorschot, M. V., Kleinhans, M., Geerling, G., & Middelkoop, H. (2016). Distinct patterns of interaction between vegetation and morphodynamics. *Earth Surface Processes and Landforms*, *41*(6), 791–808. https://doi.org/10.1002/esp.3864

Poff, N. L., & Hart, D. D. (2002). How dams vary and why it matters for the emerging science of dam removal: An ecological classification of dams is needed to characterize how the tremendous variation in the size, operational mode, age, and number of dams in a river basin influences the potential for restoring regulated rivers via dam removal. *Bioscience*, *52*(8), 659–668. https://doi.org/10.1641/0006-3568(2002)052[0659:HDVAWI]2.0.CO;2

Rinaldi, M., Wyżga, B., & Surian, N. (2005). Sediment mining in alluvial channels: Physical effects and management perspectives. *River Research and Applications*, *21*(7), 805–828. https://doi.org/10.1002/rra.884

Rivaes, R., Rodríguez-González, P. M., Albuquerque, A., Pinheiro, A. N., Egger, G., & Ferreira, M. T. (2015). Reducing river regulation effects on riparian vegetation using flushing flow regimes. *Ecological Engineering*, *81*, 428–438. https://doi.org/10.1016/j.ecoleng.2015.04.059

Serlet, A. J., Gurnell, A. M., Zolezzi, G., Wharton, G., Belleudy, P., & Jourdain, C. (2018). Biomorphodynamics of alternate bars in a channelized, regulated river: An integrated historical and modelling analysis. *Earth Surface Processes and Landforms*, *43*(9), 1739–1756. https://doi.org/10.1002/esp.4349

Solari, L., Van Oorschot, M., Belletti, B., Hendriks, D., Rinaldi, M., & Vargas-Luna, A. (2016). Advances on modelling riparian vegetation—Hydromorphology interactions. *River Research and Applications*, *32*(2), 164–178. https://doi.org/10.1002/rra.2910

Stoffel, M., & Wilford, D. J. (2012). Hydrogeomorphic processes and vegetation: Disturbance, process histories, dependencies and interactions. *Earth Surface Processes and Landforms*, *37*(1), 9–22. https://doi.org/10.1002/esp.2163

Stone, B. M., & Shen, H. T. (2002). Hydraulic resistance of flow in channels with cylindrical roughness. *Journal of Hydraulic Engineering*, *128*(5), 500–506. https://doi.org/10.1061/(ASCE)0733-9429(2002)128:5(500)

Talmon, A. M., Struiksma, N., & Van Mierlo, M. C. L. M. (1995). Laboratory measurements of the direction of sediment transport on transverse alluvial-bed slopes. *Journal of Hydraulic Research*, *33*(4), 495–517. https://doi.org/10.1080/00221689509498657

Tassi, P., Benson, T., Delinares, M., Fontaine, J., Huybrechts, N., Kopmann, R., Pavan, S., Pham, C. T., Taccone, F., & Walther, R. (2023). GAIA-a unified framework for sediment transport and bed evolution in rivers, coastal seas and transitional waters in the TELEMAC-MASCARET modelling system. *Environmental Modelling & Software*, *159*, 105544. https://doi.org/10.1016/j.envsoft.2022.105544

Van Bendegom, L. (1947). Some considerations on river morphology and river improvement. *De Ingenieur*, *59*(4), B1–B11.

Van Breen, L. E., Jesse, P., & Havinga, H. (2003). River restoration from a river manager's point of view. *Large Rivers*, *15*(1-4), 359–371. https://doi.org/10.1127/lr/15/2003/359

Vargas-Luna, A., Crosato, A., & Uijttewaal, W. S. (2015). Effects of vegetation on flow and sediment transport: Comparative analyses and validation of predicting models. *Earth Surface Processes and Landforms*, *40*(2), 157–176. https://doi.org/10.1002/esp.3633

Villada Arroyave, J. A., & Crosato, A. (2010). Effects of river floodplain lowering and vegetation cover. In *Proceedings of the Institution of Civil Engineers-water management* (Vol. 163, No. 9) (pp. 457–467). Thomas Telford Ltd. https://doi.org/10.1680/wama.900023

Webb, A. A., & Erskine, W. D. (2003). A practical scientific approach to riparian vegetation rehabilitation in Australia. *Journal of Environmental Management*, *68*(4), 329–341. https://doi.org/10.1016/S0301-4797(03)00071-9

Wilcock, P. R., & Crowe, J. C. (2003). Surface-based transport model for mixed-size sediment. *Journal of Hydraulic Engineering*, *129*(2), 120–128. https://doi.org/10.1061/(ASCE)0733-9429(2003)129:2(120)

Wintenberger, C. L., Rodrigues, S., Greulich, S., Bréhéret, J. G., Jugé, P., Tal, M., Dubois, A., & Villar, M. (2019). Control of non-migrating bar morphodynamics on survival of populus Nigra seedlings during floods. *Wetlands*, *39*(2), 275–290. https://doi.org/10.1007/s13157-018-1121-7

Yu, Q., Rennie, C. D., Slaney, J. M., & Parsapour-Moghaddam, P. (2022). Impact evaluation of instream bar management using morphodynamic modelling. *Journal of Environmental Management*, *318*, 115564. https://doi.org/10.1016/j.jenvman.2022.115564

SUPPORTING INFORMATION

Additional supporting information can be found online in the Supporting Information section at the end of this article.

How to cite this article: Li, J., Claude, N., Tassi, P., Cordier, F., Crosato, A., & Rodrigues, S. (2023). River restoration works design based on the study of early-stage vegetation development and alternate bar dynamics. *River Research and Applications*, 1–14. https://doi.org/10.1002/rra.4188